Inorg. Chem. **2005**, *44*, 3485–3493

The Reaction between ZnO and Molten $Na_2S_2O_7$ or $K_2S_2O_7$ Forming $Na_2Zn(SO_4)_2$ or $K_2Zn(SO_4)_2$, Studied by Raman Spectroscopy and X-ray Diffraction

Rolf W. Berg* and Niels Thorup

Department of Chemistry, Kemitorvet, DTU Building 207, Technical University of Denmark, DK-2800 Lyngby, Denmark

Received January 13, 2005

Reactions between solid zinc oxide and molten sodium or potassium pyrosulfates at 500 °C are shown by Raman spectroscopy to be 1:1 reactions leading to solutions. By lowering the temperature of the solution melts, colorless crystals form. Raman spectra of the crystals are given and tentatively assigned. Crystal structures of the monoclinic salts at room temperature are given. $Na_2Zn(SO_4)_2$: space group = $P2/n$ (No. 13), $Z = 8$, $a = 8.648(3)$ Å, $b = 10.323(3)$ Å, $c = 15.103(5)$ Å, $\beta = 90.879(6)°$, and $wR_2 = 0.0945$ for 2748 independent reflections. $K_2Zn(SO_4)_2$: space group = $P2_1/n$ (No.14), $Z = 4$, $a = 5.3582(11)$ Å, $b = 8.7653(18)$ Å, $c = 16.152(3)$ Å, $\beta = 91.78(3)°$, and $wR_2 = 0.0758$ for 1930 independent reflections. In both compounds, zinc is nearly perfectly trigonally bipyramidal, coordinated to five oxygen atoms, with Zn–O bond lengths ranging from 1.99 to 2.15 Å, equatorial bonds being slightly shorter on the average. The O–Zn–O angles are approximately 90° and 120°. The sulfate groups connect adjacent Zn^{2+} ions, forming complicated three-dimensional networks. All oxygen atoms belong to nearly perfect tetrahedral SO_4^{2-} groups, bound to zinc. No oxygen atom is terminally bound to zinc; all zinc oxygens are further connected to sulfur atoms (Zn–O–S bridging). In both structures, some oxygen atoms are uniquely bound to certain S atoms. The sulfate group tetrahedra have quite short (1.42–1.45 Å) terminal S–O bonds in comparison to the longer (1.46–1.50 Å) Zn-bridging S–O bonds. The Na^+ or K^+ ions adopt positions between the ZnO_5 hexahedra and the SO_4 tetrahedra, completing the three-dimensional network of the $M_2Zn(SO_4)_2$ structures. Bond distances and angles compare well with literature values. Empirical correlations between S–O bond distances and average O–S–O bond angles follow a previously found trend.

Introduction

The present work originated from a general study on metal-ore dissolution reactions for solid metal oxides by pyrosulfate melt extraction processes. We report here on the stoichiometry of dissolution reactions studied by Raman spectroscopy and the formation of $Na_2Zn(SO_4)_2$ and $K_2Zn(SO_4)_2$ crystals, which were prepared by dissolving zinc oxide in the respective molten pyrosulfates at about 500 °C followed by cooling. Raman spectroscopic evidence supports the identity of these crystals. Crystal structures of the salts are reported and discussed.

It was previously known that zinc oxide (ZnO) can be dissolved, for example, in sulfuric (H_2SO_4) and disulfuric ($H_2S_2O_7$, oleum) acids. Few modern studies have been made on the behavior of ZnO when it is dissolved in molten salt systems. Potassium pyrosulfate ($K_2S_2O_7$) is a highly versatile solvent at higher temperatures, being able to dissolve, among other things, V_2O_5,[1−4] Nb_2O_5,[5,6] Ta_2O_5,[6] and MoO_3.[7] It was unknown, however, what reaction product would form when ZnO dissolves in $K_2S_2O_7$ melts. Zn(II) is expected to form

* Author to whom correspondence should be addressed. E-mail: RWB@kemi.dtu.dk.

(1) Boghosian, S. *J. Chem. Soc., Faraday Trans.* **1998**, *94*, 3463−3469.
(2) Boghosian, S.; Borup, F.; Chissanthopoulos, A. *Catal. Lett.* **1997**, *48*, 145−150.
(3) Boghosian, S.; Chissanthopoulos, A.; Fehrmann, R. *J. Phys. Chem. B* **2002**, *106*, 49−56.
(4) Boghosian, S.; Berg, R. W. *Appl. Spectrosc.* **1999**, *53* (5), 565-571.
(5) Boghosian, S.; Borup, F.; Berg, R. W. In *Molten Salts XI*; Trulove, P. C., DeLong, H. C., Stafford, G. R., Deki, S., Eds.; The Electrochemical Society: Pennington, NJ, 1998; Vol. 98−11, pp 536−543.
(6) Borup, F.; Berg, R. W.; Nielsen, K. *Acta Chem. Scand.* **1990**, *44*, 328−331.
(7) Noerbygaard, T.; Berg, R. W.; Nielsen, K. In *Molten Salts XI*; Trulove, P. C., DeLong, H. C., Stafford, G. R., Deki, S., Eds.; The Electrochemical Society: Pennington, NJ, 1998; Vol. 98−11, pp 553−573.

10.1021/ic0500513 CCC: $30.25
Published on Web 04/12/2005

Table 1. Ampule Experiments: Relative Molar Compositions X_0(ZnO) and Relative Raman Scattering I^* and $I^{[]}$ Observed in the ZnO−$Na_2S_2O_7$ and ZnO−$K_2S_2O_7$ Systems as a Function of Composition[a]

mole ratio X_0(ZnO)	peak height I(compound, ~995 cm^{-1}) (arbitrary scale)	peak height $I(M_2S_2O_7$, ~1090 cm^{-1}) (arbitrary scale)	I^*[a]	$I^{[]a}$ $n = 1.21$(Na), 1.23(K)
		M = Na		
0.052	20	1140	3.154	3.38
0.099	60	1140	2.511	2.43
0.131	90	1220	2.037	2.49
0.180	115	885	1.691	2.30
0.372	970	970	0.592	2.09
0.380	1080	820	0.466	1.80
0.443	1125	180	0.127	3.49
		M = K		
0.110	194.20	3329.65	2.12	2.49
0.214	155.45	726.99	1.28	1.92
0.320	1637.05	2136.21	0.61	1.46
0.414	2527.33	891.18	0.25	1.89
0.428	2368.99	630.09	0.20	2.47
0.483	4006.38	114.85	0.03	
0.499	5863.50	137.30	0.02	

[a] For the meaning of symbols, see the text associated with eqs 2 and 3.

anionic sulfate complexes, and compounds such as $Na_2Zn(SO_4)_2$,[8] $Na_6Zn(SO_4)_4$,[9] $K_2Zn(SO_4)_2$,[10] and $K_2Zn_2(SO_4)_3$[11−13] have been reported to exist.

To find out more, ZnO was mixed with $Na_2S_2O_7$ or $K_2S_2O_7$ in varying molar amounts under anhydrous conditions in sealed ampules that were subsequently heated to allow for equilibration in the liquid state at about 500 °C. Raman spectra from these melts were recorded to characterize the products. From these spectra, by use of a method described in detail previously,[4] it was possible to estimate the reactions to be of the 1:1 type. By slowly cooling the melts, we were able to isolate platelike crystals suitable for X-ray structure determinations, as described in the following.

Experimental Section

Chemicals. Salts of $Na_2S_2O_7$ and $K_2S_2O_7$, being very hygroscopic, were synthesized from $Na_2S_2O_8$ and $K_2S_2O_8$ salts (both from Merck, with analyses > 99%) by thermal decomposition in dry N_2 atmospheres for 1 h at 250 °C. The products were immediately transferred to an air-filled drybox.[14] Weighed amounts of $Na_2S_2O_7$ or $K_2S_2O_7$ and ZnO (Merck, >99%) were introduced into quartz cylindrical ampules, which were subsequently sealed under vacuum. The relative molar compositions are given in Table 1. The ampules were heated in a rocking furnace at about 500 °C. All ZnO dissolved (reacted) to form viscous yellowish melts (the mp is 402 °C for $Na_2S_2O_7$ and 419 °C for $K_2S_2O_7$[15]). When cooled, the melts froze to crystalline lumps or, for high zinc contents, clear glasses. Equimolar amounts of ZnO and $Na_2S_2O_7$ or $K_2S_2O_7$ gave clear homogeneous glass masses of formulas $Na_2Zn(SO_4)_2$ or $K_2Zn(SO_4)_2$, respectively. No chemical analysis was made because the compositions were already known and the melts were homogeneous. After prolonged heatings, small attacks on the quartz walls were seen. Crystals were grown by slowly cooling the melts, at a rate of 6 °C per hour, until the start of crystallization. Ampules were broken at ambient temperature. The crystals proved to be quite stable in ambient dry air. Melting was seen to start at about 480 °C for both kinds of crystals; according to previously reported phase diagrams, $Na_2Zn(SO_4)_2$ should melt at ~480 °C and $K_2Zn(SO_4)_2$ at ~470 °C.[16]

Raman Spectra. Spectra were obtained by use of a DILOR-XY 800-mm focal length multichannel spectrometer with macro and micro entrances, Ar^+-ion laser excitation (514.5 nm, 400 mW, polarized), and a liquid-N_2-cooled CCD detector. Rayleigh scattered light was filtered off with a Kaiser holographic Super-plus-Notch filter or near the laser line with a double *pre*-monochromator. The Raman spectral resolution was from 6 to 2 cm^{-1}. Sample temperature control was achieved by means of a homemade four-window furnace or, for crystals under the microscope, by a LINKAM HFS91/TP93 cryostat/furnace stage. A sheet polarization analyzer, permitting vertically (V) or horizontally (H) polarized light to pass through the furnace horizontally, was used to obtain VV- and VH-polarized spectra. The spectra of liquids were obtained with the analyzer in orientations permitting vertically or horizontally polarized light to pass.

X-ray Diffraction. Data were collected at 21 °C on a Siemens SMART diffractometer[17] using monochromated Mo Kα radiation ($\lambda = 0.710\ 73$ Å, $\mu = 4.898$ mm^{-1}). Unit cell dimensions were refined and intensity data were reduced (corrected for Lorentz and polarization effects) by the use of the Siemens SAINT program system.[17] The structures were solved by direct methods[18] and refined by full-matrix least-squares fitting of positional and anisotropic thermal parameters.[19] Crystallographic details are given in Table 2 and in the Supporting Information.

Results

I. Raman Determination of Reaction Stoichiometry. Raman spectra of melts at ~500 °C as a function of the mole ratio, X(ZnO), among ZnO and $Na_2S_2O_7$ or $K_2S_2O_7$ are shown in Figures1 and 2. The characteristic bands of $Na_2S_2O_7$ or $K_2S_2O_7$[20,21] [bottom, X(ZnO) = 0.0000] gradually disappeared as the ZnO mole ratios increased; for example, see the disappearing of the major band of $S_2O_7^{2-}$ at ~1090 cm^{-1} (1092 and 1084 cm^{-1} for $Na_2S_2O_7$ and $K_2S_2O_7$, respectively). At the same time, new bands, for example, at ~995 cm^{-1}, appear and increase in intensity monotonically with increasing X(ZnO), indicating that reactions have occurred.

(8) Cot, M.; Tiesi, M. *C. R. Seances Acad. Sci., Ser. C* **1968**, *266*, 1159−1161.
(9) Keester, K.; Eysel, W. Inst. f. Kristallogr., Technische Hochschule, Aachen, Germany. Private communication, 1975. Cited from JCPDS-ICDD Diffraction Data File no. 29-1289.
(10) Koehler, K.; Franke, W. Mineralog. Inst., Freie University, Berlin, Germany. Private communication, 1965. Cited from JCPDS-ICDD Diffraction Data file no. 18-1073.
(11) Moriyoshi, C.; Itoh, K. *J. Phys. Soc. Jpn.* **1996**, *65*, 3537−3543.
(12) National Bureau of Standards (U.S.), Monogr. 25, **1968**, *6*, 54. Cited from JCPDS-ICDD Diffraction Data file no. 20-0957.
(13) Speer, D.; Salje, E. *Phys. Chem. Miner.* **1986**, *13*, 17−24.
(14) Hansen, N. H.; Fehrmann, R.; Bjerrum, N. J. *Inorg. Chem.* **1982**, *21*, 744−752.
(15) Rasmussen, S. B.; Eriksen, K. M.; Hatem, G.; da Silva, F.; Ståhl, K.; Fehrmann, R. *J. Phys. Chem. B* **2001**, *105*, 2747−2752.
(16) Khakhlova, N. V.; Dombrovskaya, N. S. *Zh. Neorg. Khim.* **1959**, *4*, 920−927.
(17) *SMART* and *SAINT*; Data Collection and Processing Software for the SMART System; Siemens Analytical X-ray Instruments, Inc.: Madison, WI, 1995.
(18) Sheldrick, G. M. *SHELXTL/PC*, version 5.0; Siemens Analytical X-ray Instruments, Inc.: Madison, WI, 1994.
(19) Sheldrick, G. M. *SHELXL-97*; Siemens Analytical X-ray Instruments, Inc.: Madison, WI, 1997.
(20) Dyekjaer, J. D.; Berg, R. W.; Johansen, H. *J. Phys. Chem. A* **2003**, *107* (30), 5826−5830.
(21) Fehrmann, R.; Hansen, N. H.; Bjerrum, N. J. *Inorg. Chem.* **1983**, *22*, 4009−4014.

Table 2. Crystal Data

formula	$Na_2Zn(SO_4)_2$	$K_2Zn(SO_4)_2$
mol wt/g mol^{-1}	303.47	335.69
cryst size/mm	0.30 × 0.18 × 0.01	0.13 × 0.13 × 0.01
cryst syst	monoclinic	monoclinic
space group	$P2/n$ (No. 13, C_{2h}^4)	$P2_1/n$ (No. 14, C_{2h}^5)
a/Å	8.648(3)	5.358(1)
b/Å	10.323(3)	8.765(2)
c/Å	15.103(5)	16.152(3)
β/°	90.879(6)	91.78(3)
V/Å^3	1348.05(5)	758.2(3)
D_c/g cm^{-3}	2.991	2.941
temp/K	295(2)	293(2)
Z and $F(000)$	8 and 1184	4 and 656
μ(Mo Kα)/mm^{-1}	4.40	4.898
extinction expression refined	none	$F_c^* = kF_c[1 + 0.001F_c^2\lambda^3/\sin(2\theta)]^{-1/4}$
θ range for data collection/deg	1.97−26.36	2.52−29.56
total no. of reflns	13 993 (2748 independent)	5068 (1930 independent)
reflns collected	$-10 \le h \le 10$;	$-4 \le h \le 7$;
	$-12 \le k \le 12$;	$-11 \le k \le 11$;
	$-18 \le l \le 18$	$-20 \le l \le 21$
completeness to θ	26.76°	29.56°
	100%	100%
R(int)	0.0702	0.0612
reflns with $I > 2\sigma(I)$	1741	1538
no. of params	237	119
$R_1 = \sum\|\|F_o\| - \|F_c\|\|/\sum\|F_o\|$[a]	0.0758	0.0526
	0.0369	0.0351
$wR_2 = [\sum w(F_o^2 - F_c^2)^2/\sum wF_o^4]^{1/2}$ [a]	0.0945	0.0758
	0.0810	0.0694
weight function[b]	$w^{-1} = \sigma^2(F_o^2) + (0.0399P)^2 + 0.40P$	$w^{-1} = \sigma^2(F_o^2) + (0.0342P)^2$
GOF	0.999	1.039
residual charge density/e$^-$ Å^{-3}	$-0.55 < \rho < 0.58$	$-0.8 < \rho < 0.2$

[a] For all reflections for those with $F_o^2 > 2\sigma(F_o^2)$. [b] Where $P = [\max(F_o^2,0) + 2F_c^2]/3$.

The peak intensities for these two sets of bands, above the background level of scattering, were measured in arbitrary millimeter units, I(compound, ∼995 cm^{-1}) and I($K_2S_2O_7$, ∼1090 cm^{-1}). The results are given for each melt versus the composition in Table 1. From these data, the intensity ratios between the sets of values can be calculated, and the stoichiometry n of the reaction (eq 1) be determined, by methods described in detail previously.[4]

$$ZnO + nM_2S_2O_7 \Rightarrow \text{compound (M = Na, K)} \qquad (1)$$

For the following analysis, it is convenient to define the intensity ratios I^* and $I^{[]}$ (M = Na,K):

$$I^* = \frac{I(M_2S_2O_7, \sim 1090\ \text{cm}^{-1})/X(M_2S_2O_7)}{I(\text{compound}, \sim 995\ \text{cm}^{-1})/X(\text{ZnO})} \qquad (2)$$

and

$$I^{[]} = \frac{I(M_2S_2O_7, \sim 1090\ \text{cm}^{-1})/N_{eq}(M_2S_2O_7)}{I(\text{compound}, \sim 995\ \text{cm}^{-1})/N_{eq}(\text{compound})} \qquad (3)$$

$N_{eq}(M_2S_2O_7)$ and N_{eq}(compound) are the actual mole numbers of $M_2S_2O_7$ and the new compounds, respectively, present in the scattering volume. N_{eq}(compound), for each experiment, can only be calculated after assuming a value of the stoichiometric coefficient n in the reaction (eq 1).

I^* is plotted versus X(ZnO) in Figure 3. As it can be seen, I^* extrapolates to zero for X(ZnO) = ∼0.5 (though, with some scatter), indicating that all of the $M_2S_2O_7$ has reacted at about that composition. This corresponds to a stoichiometric ratio near 1:1, and a value of n = ∼1, for both M =

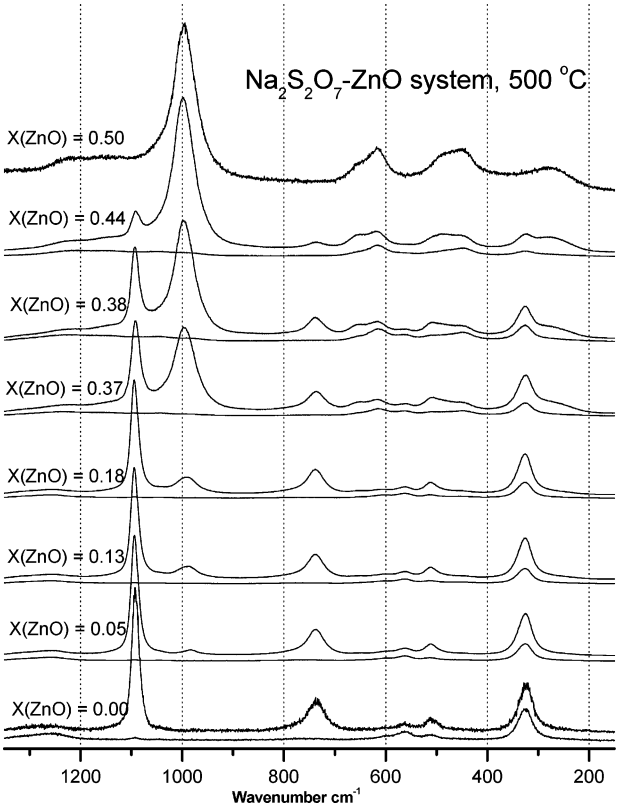

Figure 1. Raman spectra of melts at ∼500 °C as a function of composition (X = mole fraction of ZnO in the ZnO−$Na_2S_2O_7$ system). At each composition, the top spectrum is VV polarized and the bottom one is VH polarized. For $X = 0.5$, no polarization property could be observed because of scattering from undissolved particles. For $X = 0$, the VV spectrum was obtained by the suitably scaled subtraction of two different experiments to avoid visible traces of Na_2SO_4 impurities.

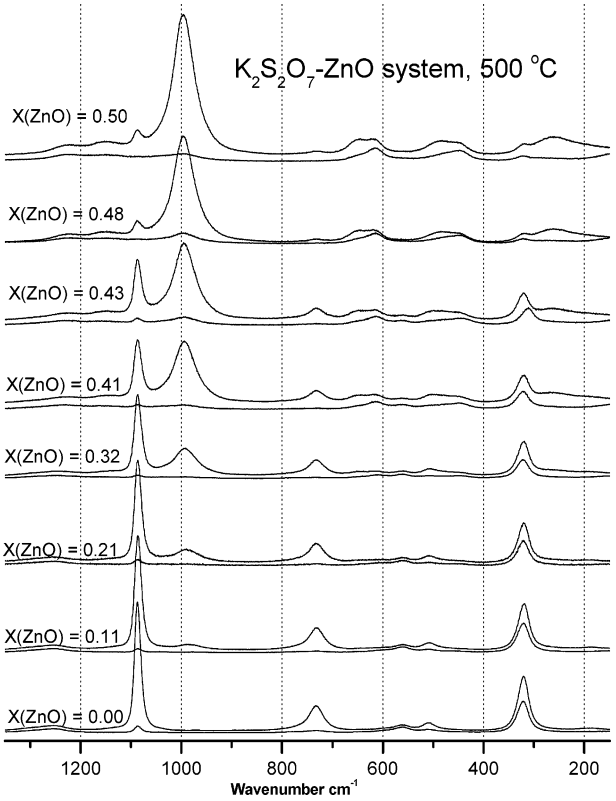

Figure 2. Raman spectra of melts at ~500 °C as a function of composition (X = mole fraction of ZnO in the ZnO−$K_2S_2O_7$ system). At each composition, the top spectrum is VV polarized and the bottom one is VH polarized.

Na and M = K. Products of formulas $Na_2Zn(SO_4)_2$ and $K_2Zn(SO_4)_2$, thus, seem to be formed. For a detailed discussion of the problems of determining n from this kind of plot, we refer to ref 4.

Alternatively, $I^{[]}$ can be calculated for assumed values of n and plotted versus X(ZnO), as in Figure 4, for n = ~1.2. The idea is that the numerator and denominator of eq 3 should each be *independent* of X(ZnO); the scattering powers *per* molecule of $M_2S_2O_7$ (numerator) and per molecule of ZnO (denominator) should be universal *constants*, apart from any M-dependence, and instrumental factors that cancel in eq 3 because both intensities were determined during the same experiment. The precision of the data, however, especially near the edges, is not as good as that of previous data, see ref 4. The $I^{[]}$ value tends to be less precise when X(ZnO) is small [N_{eq}(compound) is small] because of the unfavorable signal-to-noise ratio. In the middle of the range, $I^{[]}$ is more stable. From plots such as that in Figure 4, calculated for different values of n, we conclude that an assumption of n = ~1 seems to be the most correct one. We conclude that the products are $M_2Zn(SO_4)_2$, M = Na, K.

II. Crystal Structures. The crystal structures were solved by the direct method. Crystal data and R values are summarized in Table 2. Positional and equivalent isotropic thermal parameters, bond lengths, and angles are listed in the Supporting Information. Some selected bond lengths and angles are given in Table 3. The unit cells of the structures are shown in Figures 5 and 6.

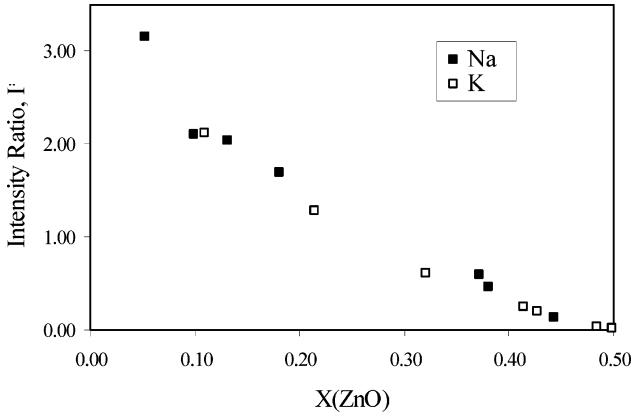

Figure 3. Plot of the Raman intensity ratio I^*, as defined in eq 2, versus the composition X(ZnO) for M = Na and K.

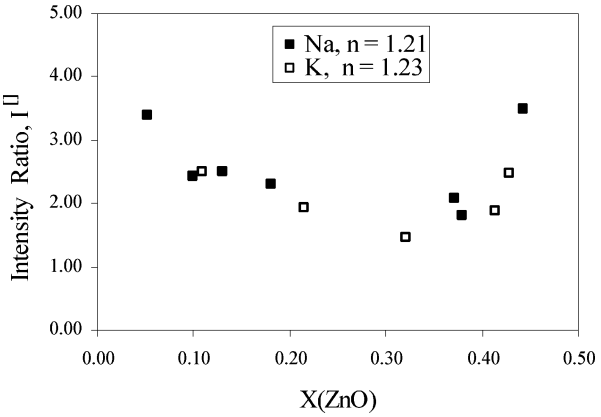

Figure 4. Plot of the Raman intensity ratio $I^{[]}$, as defined in eq 3, versus the composition X(ZnO) for M = Na and K and for assumed n values near 1. The ratio should be constant.

II.A. $Na_2Zn(SO_4)_2$. Several crystals were tried until a suitable platelike one was found (0.30 × 0.18 × 0.01 mm^3). The found structure crystallizes as described in Table 2. It contains two kinds of ZnO_5 hexahedra (bipyramids), interconnected three-dimensionally by bridging sulfate groups, see Figure 5. In the $Na_2Zn(SO_4)_2$ structure, each kind of zinc atom is coordinated to five oxygen atoms, forming nearly perfect trigonal bipyramids, see Figure 7 for an example. The coordinative Zn−O distances and their O−Zn−O angles are shown in Table 3 (three equatorial Zn1−O bonds, to O1, O9, and O14; two axial Zn1−O bonds, to O2 and O13; three equatorial Zn2−O bonds, to O4, O5, and O10; and two axial Zn2−O bonds, to O8 and O12), all of which are found to be on the order of ~2.07 ± 0.08 Å. These 2 × 5 oxygen atoms, besides being coordinated to the Zn atoms, also belong to one of the four sulfate groups (S1−S4). In the ZnO_5 hexahedra, the O−Zn1−O and O−Zn2−O angles in the triangle are 111.3°, 111.7°, and 136.5° and 110.7°, 121.6°, and 127.6°, respectively, which are at some distance from the ideal 120°, but which equate to sums of 359.5° and 359.9°, indicating near-planarity of the coordination triangles (e.g., see Figure 7). The coordinative angles between axial (O2 or O13 for Zn1 and O8 or O12 for Zn2) and equatorial oxygen atoms (O1, O9, or O14 for Zn1 and O4, O5, or O10 for Zn2) are nearly right; the three largest deviations being found for O13−Zn1−O14 (94.4°), O2−Zn1−O14 (82.0°),

Table 3. Selected Bond Distances and Angles in $Na_2Zn(SO_4)_2$ and $K_2Zn(SO_4)_2$ Structures

distances (Å)		angles (deg)		angles (deg)	
		$Na_2Zn(SO_4)_2$			
Zn1−O9	2.005(3)	O14−Zn1−O2	82.02(12)	O14−Zn1−O13	94.39(13)
Zn1−O1	2.019(3)	O1−Zn1−O13	88.47(13)	O9−Zn1−O1	111.29(13)
Zn1−O14	2.047(3)	O9−Zn1−O2	90.81(12)	O1−Zn1−O14	111.72(13)
Zn1−O13	2.063(3)	O1−Zn1−O2	91.51(12)	O9−Zn1−O14	136.52(13)
Zn1−O2	2.147(3)	O9−Zn1−O13	92.80(13)	O13−Zn1−O2	176.14(12)
Zn2−O5	1.966(3)	O5−Zn2−O12	85.17(13)	O5−Zn2−O8	94.60(13)
Zn2−O4	1.989(3)	O4−Zn2−O8	85.72(12)	O4−Zn2−O10	110.72(13)
Zn2−O10	1.992(4)	O4−Zn2−O12	90.54(13)	O5−Zn2−O10	121.57(14)
Zn2−O8	2.075(3)	O10−Zn2−O12	91.16 (14)	O5−Zn2−O4	127.57(13)
Zn2−O12	2.121(3)	O10−Zn2−O8	93.11(14)	O8−Zn2−O12	175.11(14)
S1−O3	1.434(3)	O2−S1−O4	107.46(19)	O3−S1−O2	109.89(20)
S1−O1	1.471(3)	O1−S1−O4	107.72(19)	O1−S1−O2	110.94(18)
S1−O2	1.473(3)	O3−S1−O4	109.10(19)	O3−S1−O1	111.60(21)
S1−O4	1.479(3)				
S2−O6	1.439(3)	O8−S2−O5	106.50(19)	O6−S2−O8	109.98(19)
S2−O7	1.442(3)	O6−S2−O5	108.25(18)	O7−S2−O8	110.77(21)
S2−O8	1.480(3)	O7−S2−O5	108.72(19)	O6−S2−O7	112.41(21)
S2−O5	1.509(3)				
S3−O11	1.425(3)	O10−S3−O9	107.56(19)	O11−S3−O10	109.88(22)
S3−O12	1.462(3)	O12−S3−O10	108.13(21)	O12−S3−O9	110.15(20)
S3−O10	1.466(3)	O11−S3−O12	108.84(21)	O11−S3−O9	112.20(19)
S3−O9	1.481(3)				
S4−O16	1.431(3)	O15−S4−O14	106.15(20)	O15−S4−O13	110.43(20)
S4−O15	1.456(3)	O13−S4−O14	108.17(19)	O16−S4−O14	110.85(20)
S4−O13	1.469(3)	O16−S4−O13	109.31(20)	O16−S4−O15	111.83(20)
S4−O14	1.495(3)				
		$K_2Zn(SO_4)_2$			
Zn−O3	1.997(3)	O3−Zn−O5	85.70(11)	O6−Zn−O1	93.16(10)
Zn−O6	2.018(3)	O7−Zn−O5	86.27(10)	O3−Zn−O6	109.59(11)
Zn−O1	2.045(2)	O6−Zn−O5	90.94(10)	O3−Zn−O7	112.39(11)
Zn−O7	2.050(3)	O1−Zn−O7	91.37(11)	O6−Zn−O7	137.57(11)
Zn−O5	2.086(3)	O1−Zn−O3	91.97(12)	O1−Zn−O5	175.78(11)
S1−O4	1.458(3)	O1−S1−O3	105.37(17)	O3−S1−O4	109.98(17)
S1−O2	1.460(3)	O1−S1−O2	108.64(17)	O1−S1−O4	111.29(16)
S1−O1	1.482(3)	O2−S1−O3	109.27(16)	O2−S1−O4	112.05(11)
S1−O3	1.493(3)				
S2−O8	1.460(3)	O5−S2−O6	108.09(15)	O6−S2−O8	109.62(15)
S2−O5	1.476(3)	O6−S2−O7	108.19(15)	O5−S2−O7	110.76(15)
S2−O7	1.490(3)	O7−S2−O8	109.31(17)	O5−S2−O8	110.82(16)
S2−O6	1.500(2)				

O8−Zn2−O4 (85.7°), and O12−Zn2−O5 (85.2°). The sulfate groups connect adjacent Zn^{2+} ions, forming a complicated three-dimensional network. Chained bond examples are O9−Zn1−O14−S4−O13−Zn1−O9 partly along *c* and Zn2−O10−S3−O13−Zn2−O5 partly along *a* as well as S2−O5−Zn2−O13−S4−O14−Zn1−O9−S3−O12−Zn2 and Zn1−O9−S3−O10−Zn2. All oxygens are connected to sulfur atoms, but only 10 are bound to zinc. Hence, six O atoms are uniquely bound to certain S atoms: O3 to S1, O6 and O7 to S2, O11 to S3, and O15 and O16 to S4. The sulfate groups form rather perfect tetrahedra, but the terminal S−O bonds are quite short (from ∼1.42 to ∼1.45 Å) in comparison to the bridging S−O bonds (from ∼1.46 to ∼1.50 Å), see Table 3. The Na^+ ions adopt places between the ZnO_5 hexahedra and the SO_4 tetrahedra, thus completing the $Na_2Zn(SO_4)_2$ structure.

II.B. $K_2Zn(SO_4)_2$. The structure was solved by the direct method to give the results described in Table 2. Similar results were obtained from two crystals of about 0.13 × 0.13 × 0.01 mm^3. The structure contained ZnO_5 hexahedra (bipyramids), interconnected three-dimensionally by bridging sulfate groups, see Figure 6. Also in the $K_2Zn(SO_4)_2$ structure, the zinc atom is coordinated to five oxygen atoms, forming a nearly perfect trigonal bipyramid (see the figure in the Supporting Information). The coordinative Zn−O distances and their O−Zn−O angles are shown in Table 3 (three equatorial Zn−O bonds, to O3, O6, and O7, and two axial Zn−O bonds, to O1 and O5), all of which are found to be on the order of ∼2.04 ± 0.05 Å. All oxygen atoms coordinated to Zn also belong to one of the two sulfate groups (S1 and S2). In the ZnO_5 hexahedron, the O−Zn−O angles in the triangle are 109.6°, 112.4°, and 137.6°, which are at some distance from the ideal 120°, but which equate to a sum of 359.5°, indicating near-planarity of the coordination triangle. The coordinative angles between axial (O1 or O5) and equatorial (O3, O6, or O7) oxygen atoms are nearly right; the three largest deviations are found for O5−Zn−O3 (85.7°), O5−Zn−O7 (86.3°), and O1−Zn−O6 (93.15°). The sulfate groups connect adjacent Zn^{2+} ions, forming a three-dimensional network, along *a* via O7−S2−O6 bridges, along *b* via O1−S1−O3 bridges, and along *c via* O6−S2−O5−Zn−O1−S1−O3 bridges. The sulfate groups form rather perfect tetrahedra. S1 has two oxygen atoms of its own (O4 and O2), and S2 has one (O8) of its own; these three oxygen atoms are not bound to zinc at all. This must be the reason that these terminal S−O bonds are quite short (∼1.46 Å) in comparison to the bridging S−O bonds (from ∼1.48 to ∼1.50 Å), see Table 3. The K^+ ions occupy places between

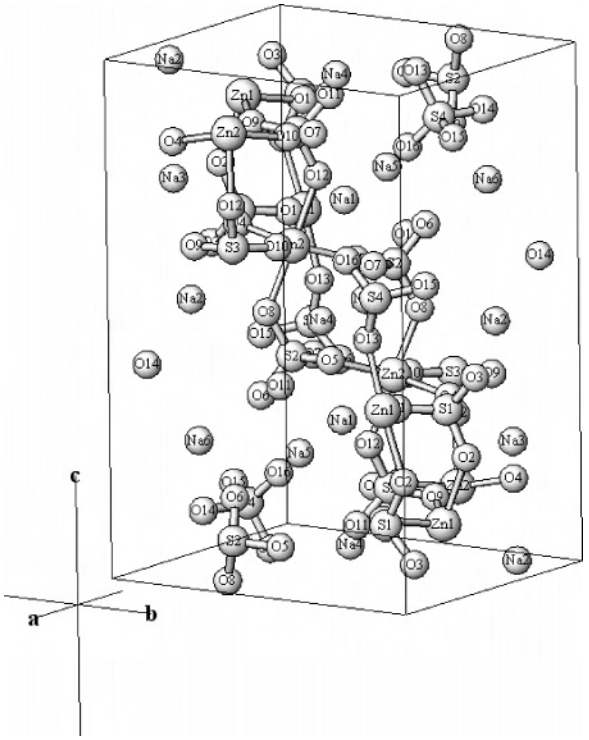

Figure 5. Unit cell of the $Na_2Zn(SO_4)_2$ structure, consisting of ZnO_5 hexahedra, interconnected three-dimensionally by bridging sulfate groups placed between sodium ions.

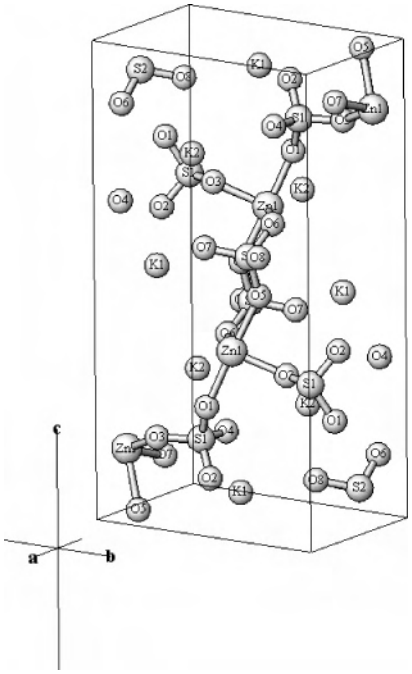

Figure 6. Unit cell of the $K_2Zn(SO_4)_2$ structure, consisting of ZnO_5 hexahedra, interconnected three-dimensionally by bridging sulfate groups placed between potassium ions.

the ZnO_5 hexahedra and the SO_4 tetrahedra, thus completing the $K_2Zn(SO_4)_2$ structure.

II.C. Discussion. Standard Zn−O distances, of coordination number 6, can be expected within 2.02−2.24 Å, and values between 2.05 and 2.11 Å have indeed been found for distorted ZnO_6 octahedra in Langbeinite-type $K_2Zn_2(SO_4)_3$ crystals.[11,13] No other crystal structure of zinc with sulfate

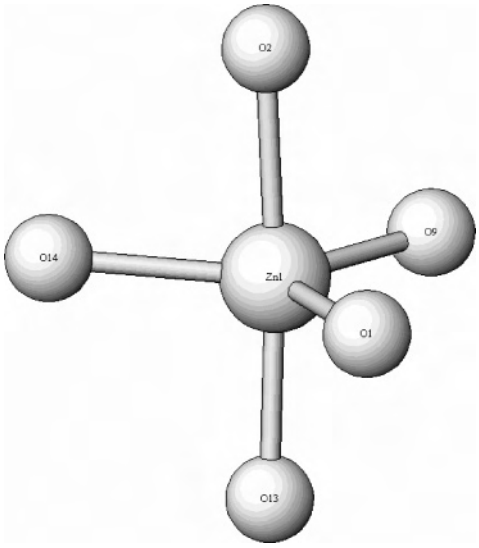

Figure 7. Geometry of the $Zn1O_5$ hexahedron in the $Na_2Zn(SO_4)_2$ structure. For the $Zn2O_5$ hexahedron, see the Supporting Information.

coordination seems to have been reported. This is the first time ever that trigonal bipyramidal arrangements of five oxide ligands around Zn have been found. Occasionally, pentacoordination has been seen in crystal structures when other non-oxide coordinate or multidentate ligands chelate to Zn; in such cases, Zn−O distances have been determined, varying from short ones (around 1.973, 1.994, and 2.035 Å; see, e.g., refs 22 and 23) to longer ones (around 2.142 Å[24]). Our found Zn−O distances all fall within the unified range ∼2.07 ± 0.08 Å, agreeing quite well with these reported values.

II.D. Distance Mean Angle Correlation in Sulfate Groups. Sulfate groups, in general, can have from zero to four oxygen atoms forming covalent bridges to other elements. If O′ is such a bridging oxygen atom, the S−O′ distance is often significantly longer than other nonbridging (or terminal) S−O distances. Also, the O−S−O angles involving terminal oxygen atoms are often significantly larger than the ideal tetrahedral angle; especially, O6−S2−O7 (Na) and O2−S1−O4 (K), among two terminal S−O bonds, are large (112.41 and 112.05°), see Table 3. The nearly tetrahedral angles are deformed because of repulsion from the short-bonded oxygen atoms. The O−S−O angles involving an oxygen atom bridging to Zn are smaller than the ideal tetrahedral angle of 109.47°. The O−S−O angles not involving bridging O atoms had enlarged values above 109.47°. The S−O distances depended on the angles such that the larger the average of the three possible O−S−O angles around a particular S−O bond, the smaller the S−O distance.

An approximately linear correlation has been empirically found between the *average* of the three sulfate O−S−O

(22) Wu, H.; Ying, W.; Pen, L.; Gau, Y.; Yu, K. *Synth. .React. Inorg. Met.-Org. Chem.* **2004**, *34* (6), 1019−1030.
(23) Bertels, J.; Mattes, R. *Z. Naturforsch*. **1985**, *40b*, 1068−1072. Note a printing error in Table 3 for the Zn−O6 distance, which should be 2.133 Å.
(24) Yang, F.-A.; Chen, J.-H.; Hsieh, H.-Y.; Elango, S.; Hwang, L.-P. *Inorg. Chem*. **2003**, *42* (15), 4603−4609.

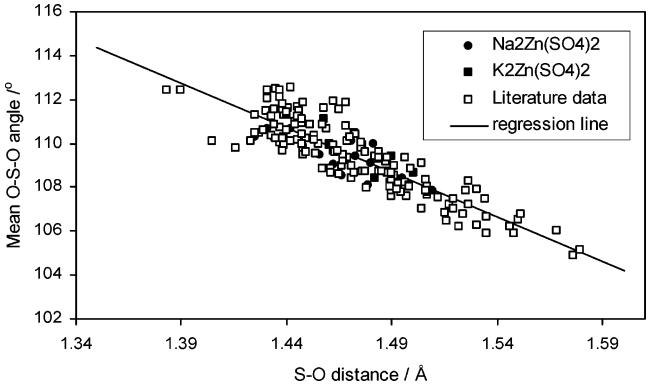

Figure 8. Plot of S−O distances for a particular bond versus the average of the three angles involving that bond and the other S−O bonds of the sulfate tetrahedron (24 solid points). The other points shown are taken from structures on $KV(SO_4)_2$,[25] $K_4(VO)_3(SO_4)_5$,[26] $Na_2VO(SO_4)_2$,[27] $NaV(SO_4)_2$,[28] $Cs_4(VO)_2(\mu\text{-}O)(SO_4)_4$,[29] $CsV(SO_4)_2$,[30] $Na_3V(SO_4)_3$,[31] β-$VOSO_4$,[32] $K_6(VO)_4(SO_4)_8$,[33] $Na_8(VO)_2(SO_4)_6$,[34] $Na_2K_6(VO)_2(SO_4)_7$,[35] $CsVO_2SO_4$,[36] $K_7Nb(SO_4)_6$,[6] $K_7Ta(SO_4)_6$,[6] and $K_2MoO_2(SO_4)_2$ [7]. The regression line ($y = ax + b$, y = mean O−S−O angle in degrees; x = S−O distance, in Å; $a = -40.825°/Å$; $b = 169.51°$) was obtained using all 177 points.

angles involving a particular bond between S and O (nonbridging as well as bridging) and the *length* of that particular S−O bond. The relationship has been found to be valid for a number of vanadium sulfates[25−36] as well as for sulfates of Nb, Ta,[6] and Mo,[7] and it is probably valid for many others. A plot of the relationship is given in Figure 8, showing the 24 new points combined with previous results, 16 for $Na_2Zn(SO_4)_2$ and 8 for $K_2Zn(SO_4)_2$. Obviously, the new points, as expected, fit very well within the plot. The relationship in Figure 8 indicates a general trend between bond distances and hybridization of the central tetrahedral sulfur atom.

II.E. Bond Length/Bond Strength Correlations. The obtained bond distances (Table 3 and Supporting Information) were used to determine bond orders by the method of correlation. On the basis of the crystal structure data of many compounds, Brown and co-workers[37−39] have developed general nonlinear relationships between the atom-to-oxygen bond valence, s, and the atom-to-oxygen bond distance R. An empirical expression relating the A−O distance to the bond valence (A is an atom, here, Zn, S, Na, or K) is

$$s(\mathrm{A-O}) = s_o(R/R_1)^{-N} \qquad (4)$$

where s_o, R_1, and N are empirical constants. From calculated values for the bond orders around an atom, the oxidation state can be estimated by summation. In this way, we were able to reproduce, satisfactorily, the formal valence of the atoms. Zn, S, Na, K, and O come out in the +2, +6, +1, +1, and −2 oxidation states, respectively, see Table 4 (the full set of data is given in the Supporting Information). Our structural results, thus, fit into the general results given in the literature.[37,38] Such a fit should provide a vice versa test of the plausibility of the method of bond order summation and the crystal structure solutions if the sum lies within 5% of the formal oxidation state.[37]

Table 4. Empirical Bond Orders ($s = s_o(R/R_1)^{-N}$) for Zn and S and Bond Order Sums ($\sum s$) for All Atoms Based on Bond Distances R' [a]

$Na_2Zn(SO_4)_2$				$K_2Zn(SO_4)_2$	
bond	bond order s^b	bond	bond order s^b	bond	bond order s^b
Zn1−O9	0.43	Zn2−O5	0.49	Zn−O3	0.44
Zn1−O1	0.42	Zn2−O4	0.45	Zn−O6	0.42
Zn1−O14	0.38	Zn2−O10	0.45	Zn−O1	0.38
Zn1−O13	0.36	Zn2−O8	0.35	Zn−O7	0.38
Zn1−O2	0.29	Zn2−O12	0.31	Zn−O5	0.34
$\sum s^c$ Zn1	1.88 ± 0.05	$\sum s^c$ Zn2	2.05 ± 0.05	$\sum s^c$ Zn	1.96 ± 0.03
S1−O3	1.64	S3−O11	1.68	S1−O4	1.53
S1−O1	1.48	S3−O12	1.52	S1−O2	1.52
S1−O2	1.47	S3−O10	1.50	S1−O1	1.44
S1−O4	1.45	S3−O9	1.44	S1−O3	1.39
$\sum s^c$ S1	6.04 ± 0.05	$\sum s^c$ S3	6.14 ± 0.05	$\sum s^c$ S1	5.89 ± 0.05
S2−O6	1.62	S4−O16	1.65	S2−O8	1.53
S2−O7	1.60	S4−O15	1.54	S2−O5	1.46
S2−O8	1.44	S4−O13	1.49	S2−O7	1.41
S2−O5	1.34	S4−O14	1.39	S2−O6	1.37
$\sum s^c$ S2	6.00 ± 0.06	$\sum s^c$ S4	6.07 ± 0.06	$\sum s^c$ S2	5.76 ± 0.05
$\sum s^c$ Na1	0.98 ± 0.06	$\sum s^c$ Na4	1.01 ± 0.06	$\sum s^c$ K1	0.92 ± 0.06
$\sum s^c$ Na2	1.07 ± 0.01	$\sum s^c$ Na5	0.90 ± 0.06	$\sum s^c$ K2	1.00 ± 0.06
$\sum s^c$ Na3	1.00 ± 0.06	$\sum s^c$ Na6	0.83 ± 0.06	$\sum s^c$ O1	2.00 ± 0.06
$\sum s^c$ O1	1.90 ± 0.06	$\sum s^c$ O9	1.96 ± 0.06	$\sum s^c$ O2	1.88 ± 0.06
$\sum s^c$ O2	1.95 ± 0.06	$\sum s^c$ O10	2.17 ± 0.06	$\sum s^c$ O3	1.89 ± 0.06
$\sum s^c$ O3	1.99 ± 0.06	$\sum s^c$ O11	2.00 ± 0.06	$\sum s^c$ O4	1.90 ± 0.06
$\sum s^c$ O4	2.20 ± 0.06	$\sum s^c$ O12	2.02 ± 0.06	$\sum s^c$ O5	1.92 ± 0.06
$\sum s^c$ O5	2.03 ± 0.06	$\sum s^c$ O13	2.04 ± 0.06	$\sum s^c$ O6	1.97 ± 0.06
$\sum s^c$ O6	2.03 ± 0.06	$\sum s^c$ O14	2.00 ± 0.06	$\sum s^c$ O7	1.98 ± 0.06
$\sum s^c$ O7	1.91 ± 0.06	$\sum s^c$ O15	1.93 ± 0.06	$\sum s^c$ O8	1.84 ± 0.06
$\sum s^c$ O8	2.01 ± 0.06	$\sum s^c$ O16	1.90 ± 0.06		

[a] s_o, R_1, and N are literature parameters. [b] Bond order estimated precision is better than ±0.005 to ±0.02. For Zn^{2+}, the universal 28-electron expression of Brown and Shannon[37] was used: $s = (R/1.746\ Å)^{-6.050}$. This expression was derived on the basis of 29 zinc-containing selected crystal structure determinations. For S^{6+}, Na^+, and K^+, the expressions $s(S^{6+}) = 1.5(R/1.466\ Å)^{-4.00}$, $s(Na^+) = 0.166(R/2.421)^{-5.7}$, and $s(K^+) = 0.125(R/2.833)^{-5.0}$ were used.[37] The oxygen sums are based on the same expressions. [c] Each sum is an estimation of the oxidation state of the atom.

III. Vibrational Spectra. A. Expectations. The internal vibrations of a regular, free SO_4^{2-} ion of T_d symmetry span

(25) Fehrmann, R.; Krebs, B.; Papatheodorou, G. N.; Berg, R. W.; Bjerrum, N. J. *Inorg. Chem.* **1986**, *25*, 1571−1577.
(26) Fehrmann, R.; Boghosian, S.; Papatheodorou, G. N.; Nielsen, K.; Berg, R. W.; Bjerrum, N. J. *Inorg. Chem.* **1989**, *28*, 1847−1853.
(27) Fehrmann, R.; Boghosian, S.; Papatheodorou, G. N.; Nielsen, K.; Berg, R. W.; Bjerrum, N. J. *Inorg. Chem.* **1990**, *29*, 3294−3298.
(28) Fehrmann, R.; Boghosian, S.; Papatheodorou, G. N.; Nielsen, K.; Berg, R. W.; Bjerrum, N. J. *Acta Chem. Scand.* **1991**, *45*, 961−964.
(29) Nielsen, K.; Fehrmann, R.; Eriksen, K. M. *Inorg. Chem.* **1993**, *32*, 4825−4828.
(30) Berg, R. W.; Boghosian, S.; Bjerrum, N. J.; Fehrmann, R.; Krebs, B.; Sträter, N.; Mortensen, O. S.; Papatheodorou, G. N. *Inorg. Chem.* **1993**, *32*, 4714−4720 and corrections in *Inorg. Chem.* **1994**, *33*, 402.
(31) Boghosian, S.; Fehrmann, R.; Nielsen, K. *Acta Chem. Scand.* **1994**, *48*, 724−731.
(32) Boghosian, S.; Eriksen, K. M.; Fehrmann, R.; Nielsen, K. *Acta Chem. Scand.* **1995**, *49*, 703−708.
(33) Eriksen, K. M.; Nielsen, K.; Fehrmann, R. *Inorg. Chem.* **1996**, *35*, 480−484. Note that some points are in error in the angle-distance plot, Figure 2.
(34) Nielsen, K.; Boghosian, S.; Fehrmann, R.; Berg, R. W. *Acta Chem. Scand.* **1999**, *53*, 15−23.
(35) Karydis, D. A.; Boghosian, S.; Nielsen, K.; Eriksen, K. M.; Fehrmann, R. *Inorg. Chem.* **2002**, *41*, 2417−2421.
(36) Rasmussen, S. B.; Boghosian, S.; Nielsen, K.; Eriksen, K. M.; Fehrmann, R. *Inorg. Chem.* **2004**, *43*, 3697−3701.
(37) Brown, I. D.; Shannon, R. D. *Acta Crystallogr., Sect. A* **1973**, *A29*, 266−282.
(38) Brown, I. D.; Wu, K. K. *Acta Crystallogr., Sect B* **1976**, *B32*, 1957−1959.
(39) Brown, I. D. In *Structure and Bonding in Crystals*; O'Keeffe, M., Navrotsky, A., Eds.; Academic Press: New York, 1981; Vol. II, Chapter 14, pp 1−30.

Table 5. Correlation Diagram for the Internal Vibrations in the SO_4^{2-} Ions in the Unit Cell of $K_2Zn(SO_4)_2$[a]

8 Isolated ions of T_d point group symmetry	8 ions on sites of no symmetry	8 ions in a crystal of C_{2h}^5 Factor group symmetry
		18 A_g ν_1 (str), ν_2 (bend), ν_3 (str), ν_4 (bend) Raman activity: x^2, y^2, z^2, xy
8 A_1 ν_1 (str) Raman activity:$x^2+y^2+z^2$		18 B_g ν_1 (str), ν_2 (bend), ν_3 (str), ν_4 (bend) Raman activity: xz, yz
8 E ν_2 (bend) Raman activity: $2z^2-x^2-y^2$, x^2-y^2	72 A	18 A_u ν_1 (str), ν_2 (bend), ν_3 (str), ν_4 (bend) IR activity: z
18 F_2 ν_3 (str), ν_4 (bend) Raman activity: xz, yz, xy IR activity: x, y, z		18 B_u ν_1 (str), ν_2 (bend), ν_3 (str), ν_4 (bend) IR activity: x, y

[a] Code: ν_1(str), ν_2(bend), ν_3(str), and ν_4(bend) are the A_1, E, and $^2F_2$ stretching and bending mode components of the SO_4^{2-} group under T_d symmetry.

Table 6. Factor Group Analysis[a] for $K_2Zn(SO_4)_2$ Crystallizing in Space Group C_{2h}^5 ($P2_1/n$, No. 14, $Z = 4$)

		← optically active normal modes →			
	T_a	T	$R(SO_4^{2-})$	$N_i(SO_4^{2-})$	activity in
A_g		15	6	18	Raman: x^2, y^2, z^2, xy
B_g		15	6	18	Raman: xy, yz
A_u	1	14	6	18	IR: z
B_u	2	13	6	18	IR: x, y
total	3	57	24	72	156 degrees of freedom

[a] The *primitive* unit cell contains four formula units of 13 atoms each, that is, a total of 52 atoms. The T and R classifications are based on the same cell considered as containing eight K^+ ions, four Zn^{2+} ions, and eight SO_4^{2-} ions on Wyckoff sites e with no site symmetry. T_a = optically inactive acoustic modes, T = optic branch translatory modes of the 20 ions ($T + T_a = 3 \times 20$), $R(SO_4^{2-})$ = rotatory modes, and $N_i(SO_4^{2-})$ = internal vibrational modes of the eight SO_4^{2-} ions.

the representation $A_1(\nu_1) + E(\nu_2) + 2F_2(\nu_3 + \nu_4)$. All symmetry species are Raman, and the F_2 ones are IR observable. The fundamental modes are bond stretchings ($\nu_1 \cong 983$ cm^{-1} and $\nu_3 \cong 1105$ cm^{-1}) and mostly angle bendings within the SO_4^{2-} tetrahedron ($\nu_2 \cong 450$ cm^{-1} and $\nu_4 \cong 611$ cm^{-1}).[40−42] The coordination of sulfate to cations (in casu Zn^{2+}) decreases the symmetry, splits the degenerate modes, and relaxes the selection rules. The atoms in the *primitive* unit cells perform vibrations, which are distributed on the symmetry species of the cell. Under the C_{2h} factor group symmetry, in the common wave vector $\mathbf{k} \cong 0$ approximation,[43,44] spanning the representations $78A_g + 78B_g + 78A_u + 78B_u$ for $Na_2Zn(SO_4)_2$ and $39A_g + 39B_g + 39A_u + 39B_u$ for $K_2Zn(SO_4)_2$. The gerade species are Raman and the ungerade ones are IR permitted, except for three acoustic modes for each salt.

(40) Nakamoto, K.; *Infrared and Raman Spectra of Inorganic and Coordination Compounds*, Part A; Wiley: New York, 1997; pp 62−63, 189, 210. Nakamoto, K.; *Infrared and Raman Spectra of Inorganic and Coordination Compounds*, Part B; Wiley: New York, 1997; p 79.

(41) Hester, R. E.; Krishnan, K. *J. Chem. Phys*. **1968**, *49*, 4356−4360.

(42) Hapanowicz, R. P.; Condrate, R. A., Sr. *Spectrosc. Lett.* **1996**, *29* (1), 131−141.

(43) Rousseau, D. L.; Bauman, R. P.; Porto, S. P. S. *J. Raman Spectrosc.* **1981**, *10*, 253−290 and references therein.

(44) Adams, D. M.; Newton, D. C. *Tables for Factor Group and Point Group Analysis*; Beckman-RIIC Limited: England, 1970.

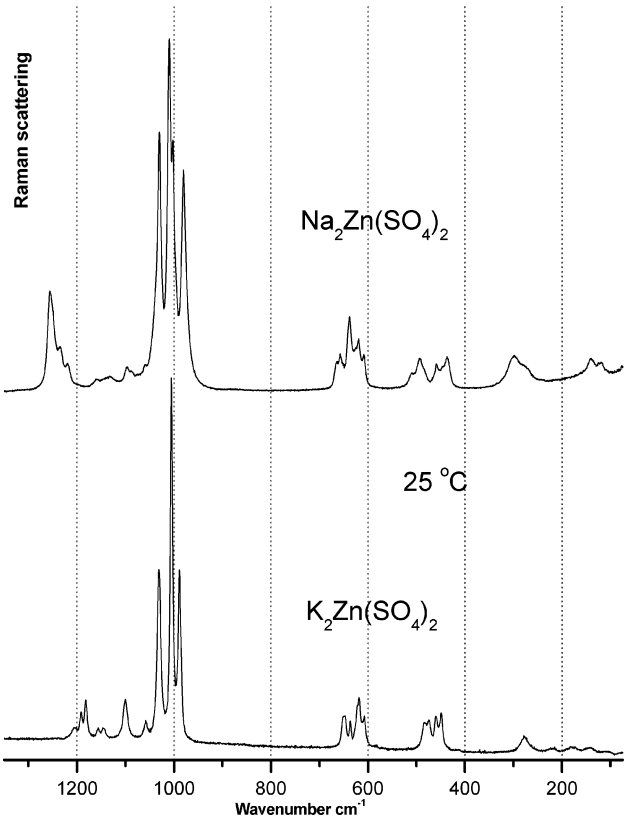

Figure 9. Raman spectra from polycrystalline samples of $Na_2Zn(SO_4)_2$ and $K_2Zn(SO_4)_2$ kept in a small box with a dry atmosphere and a quartz window. The spectra were obtained under the microscope at room temperature. The spectral resolution was ~4 cm^{-1}.

In the simplest $K_2Zn(SO_4)_2$ salt, the eight SO_4^{2-} ions (four S1 and four S2) in the primitive unit cell *each* contribute nine internal degrees of vibrational freedom (inherent in the T_d sulfate modes $\nu_1-\nu_4$), resulting in a total of 72 internal sulfate modes. These are also distributed on the symmetry species of the cell, spanning internal vibrations under the representation (distributed evenly over the symmetry types of the factor group). Some of these modes are stretchings (ν_1) and some are mixtures of stretchings and bendings (ν_3, ν_2, and ν_4), see the correlation diagram given in Table 5, correlating the sulfate modes from the free to the bound state. Further, there are 24 rotational modes of the eight SO_4^{2-} ions and 60 translations of the four Zn^{2+}, eight K^+, and eight SO_4^{2-} ions, three of which are optically inactive acoustic modes. These 72 + 24 + 60 modes, in total 156, are evenly distributed on the A_g, B_g, A_u, and B_u symmetry species (Table 6).

The primitive cell of the larger $Na_2Zn(SO_4)_2$ structure contains 16 SO_4^{2-} ions (four of each of S1−S4) that *each* contribute nine internal degrees of vibrational freedom (inherent in the T_d sulfate modes $\nu_1-\nu_4$), resulting in a total of 144 internal sulfate modes. The correlation diagram is even more numerous, without mentioning the 48 rotational modes of the 16 SO_4^{2-} ions and the 120 translations of the 8 Zn, 16 Na, and 16 SO_4^{2-} ions, three of which are optically inactive acoustic modes. These 144 + 48 + 120 modes, in total 312, are evenly distributed on the A_g, B_g, A_u, and B_u symmetry species.

Table 7. Raman Bands (in cm^{-1}) and Approximate Assignments[a]

$Na_2Zn(SO_4)_2$		$K_2Zn(SO_4)_2$		
Raman, crystal at 25 °C	Raman melt at 500 °C	Raman, crystal at 25 °C	Raman melt at 500 °C	tentative assignments
1255 m		1205 vw		
1235 w	1225 wbr, p	1192 w	1225 wbr, p	
1219 vw		1182 w		ν_3(str, SO_4^{2-})
1160 vw	1150 w, br	1156 vw	1150 w, br	ν_3(str, SO_4^{2-})
1130 vw		1146 vw		ν_3(str, SO_4^{2-})
1095 w		1101 m		
			1086 w, p	$K_2S_2O_7$ traces
1058 vw		1058 w		ν_3(str, SO_4^{2-})
1029 vs		1031 s		ν_1(str, SO_4^{2-})
1009 vs		1005 vs		ν_1(str, SO_4^{2-})
1002 s	996 vs, p	989 s	995 vs, p	ν_1(str, SO_4^{2-})
980 s				ν_1(str, SO_4^{2-})
			732 vw, p	$K_2S_2O_7$ traces
664 vw				ν_4(bend, SO_4^{2-})
657 w	658 w, p	650 m br	650 w, p	ν_4(bend, SO_4^{2-})
637 m		636 w		ν_4(bend, SO_4^{2-})
620 w	616 m, dp	620 m	616 m, dp	ν_4(bend, SO_4^{2-})
608 vw		608 w		ν_4(bend, SO_4^{2-})
509 vw	487 w, p	483 w	485 w, p	ν_2(bend, SO_4^{2-})
492 w		474 w		ν_2(bend, SO_4^{2-})
458 w	451 w, dp	460 w	450 w, dp	ν_2(bend, SO_4^{2-})
436 w		449 w		ν_2(bend, SO_4^{2-})
			321 w, dp	$K_2S_2O_7$ traces
297 w		277 w		ν(Zn−OSO_3^{2-})
275 w, br	270 wbr, p		261 wbr, p	ν(Zn−OSO_3^{2-})
		220 vw		ν(Zn−OSO_3^{2-})
140 w		178 vw		$\nu_{lattice}$
120w		144 vw		$\nu_{lattice}$
		108 vw		$\nu_{lattice}$

[a] Intensity codes: w = weak, m = medium, s = strong, sh = shoulder, v = very, br = broad, p = polarized, and dp = depolarized. Calibration with neon lines to a precision of 1 cm^{-1}.

The ZnO_5 core with its approximate D_{3h} symmetry should, if alone, give Raman active modes according to two A'_1 (stretchings) and three $E' + E''$ (bendings) modes.

III.B. Interpretation. Observed Raman spectra are shown in Figure 9, and band positions given in Table 7. As it can be seen, the observed spectra contain much fewer bands than predicted above. Characteristic SO_4^{2-} stretchings were assigned to bands in the range from ~900 to 1300 cm^{-1}. In the range of SO_4^{2-} angle bending (~400−700 cm^{-1}), the many observed bands are difficult to assign definitively, because extensive couplings must exist among most of the modes because of the low symmetry and the near coincidence of the frequencies. Zn−O stretchings and O−Zn−O deformations are probably contained in bands near 200−300 cm^{-1}. Below that, lattice modes due to the anion−cation vibration should be expected. It is interesting to note that in aqueous $ZnSO_4$ solutions (both for H_2O and D_2O), Zn−O ligand vibrations have been found at 275−282 cm^{-1} as a result of inner sphere $Zn^{2+}SO_4^{2-}$ complex ions present in the solutions.[45,46] Some minor bands may be due to traces of $Na_2S_2O_7$ or $K_2S_2O_7$.

Acknowledgment. Support from several Danish foundations made the purchase of the DILOR Raman instrument and its accessories possible: The Danish Technical Science Foundation, Corrit Foundation, Tuborg Brewery Foundation, Danfoss A/S, Thomas B. Thrige Foundation, P. A. Fiskers Foundation, and Direktør Ib Henriksens Foundation. Also, help was received from Kurt Nielsen, Steen Blichfeldt, and Bodil Holten of DTU. Soghomon Boghosian of FORTH/ICE-HT, Patras University, Greece, is thanked for valuable discussions.

Supporting Information Available: X-ray crystallographic details in CIF format and further information in PDF format. This material is available free of charge via the Internet at http://pubs.acs.org.

IC0500513

(45) Rudolph, W.; Brooker, M. H.; Tremaine, P. *Z. Phys. Chem.* **1999**, *209*, 181−207.
(46) Rudolph, W.; Brooker, M. H.; Tremaine, P. *J. Solution Chem.* **1999**, *28* (5), 621−630.